Materials Research Bulletin 48 (2013) 58–62

Contents lists available at SciVerse ScienceDirect

Materials Research Bulletin

journal homepage: www.elsevier.com/locate/matresbu

Effect of silver addition on the microstructures and electrical responses of La(1.7)Sr(0.3)Mo(2)O(9 − δ) ceramics

Xiao Liu, Huiqing Fan *, Jing Shi

State Key Laboratory of Solidification Processing, School of Materials Science and Engineering, Northwestern Polytechnical University, Xi'an 710072, China

ARTICLE INFO

Article history:
Received 30 June 2012
Received in revised form 14 September 2012
Accepted 1 October 2012
Available online 10 October 2012

Keywords:
A. Oxides
C. Impedance spectroscopy
D. Diffusion
D. Ionic conductivity

ABSTRACT

Different amounts of silver (3–15 wt.% Ag_2O) have been mixed with ceramic powders based on $La_{1.7}Sr_{0.3}Mo_2O_{9-\delta}$ (LSM). XRD analysis indicated that the silver was chemically stable in LSM. TEM observation and XPS analysis showed that some metallic silver atoms presented random distribution in the LSM ceramic, while others entered into crystal lattice in the form of Ag^+, efficiently stabilizing the cubic phase at the room temperature. And there were a great enhancement on conductivity in Ag added (<10 wt.% Ag_2O) LSM ceramics. Also addition of Ag had a significant influence on the surface oxygen exchange properties with electrode components.

1. Introduction

The discovery, in $La_2Mo_2O_9$ (LM), of an oxide-ion conductivity higher than that of stabilized zirconias above 580 °C opened the prospect for using this material as a promising electrolyte material in solid oxide fuel cells (SOFCs) [1,2]. It is well known that this material undergoes a phase transition from monoclinic α-$La_2Mo_2O_9$ at low temperature to cubic β-$La_2Mo_2O_9$ at high temperature associated with a sharp jump in ionic conductivity. Studies of the crystal structure have shown that the nature of the phase transition is a change of the distribution of oxygen defects [2–6]. The oxygen transport mechanism changes with the phase transition from a thermally activated Arrhenius type at low temperature to a thermally assisted VTF (Vogel–Tamman–Fulcher) type [7,8]. Numerous works were devoted to stabilizing the high-T cubic β-form to lower temperatures through solid solution formation (derivatives of $La_2Mo_2O_9$, the so-called LAMOX family) to enhance the oxide ion conductivity below the first order transition [9–12].

Ceramic metal composites have attracted much attention due to their unique properties, which are different from the properties of constituent components. The corresponding percolation threshold theory has been established. With the addition of metals in ceramics, the same electric field can induce higher polarization and produce much greater conductivity [13–15]. As well, silver has been noted as a good catalyst for the electrochemical reduction of oxygen in Ag/electrolyte systems. The application of silver to enhance the surface oxygen exchange for diffusion in ionic conductors has already been demonstrated [16–18]. As previous study, the Sr doping in LMO has a positive influence on oxide ion conductivity. By contrast, we choose the $La_{1.7}Sr_{0.3}Mo_2O_{9-\delta}$ as the primary reactant. In the present work, the effects of different silver (3–18 wt.% Ag_2O) addition on the phase constitution, microstructure, and electrical responses properties of $La_{1.7}Sr_{0.3}Mo_2O_{9-\delta}$ ceramics were investigated.

2. Experimental procedure

$La_{1.7}Sr_{0.3}Mo_2O_{9-\delta}$ composites with 3, 5, 8, 10, 12, 15, 18 wt.% Ag_2O (respectively, labeled with 3Ag, 5Ag, 8Ag, 10Ag, 12Ag, 15Ag, 18Ag) were prepared by the conventional solid state ceramic route. First, powder samples of $La_{1.7}Sr_{0.3}Mo_2O_{9-\delta}$ were prepared by the conventional mixed-oxide technique. The starting reactants were analytical grade La_2O_3 (purity ≥ 99.5%), $SrCO_3$ (purity ≥ 99%) and MoO_3 (purity ≥ 99.5%), which were weighted according to the composition. Prior to use, La_2O_3 was calcinated at 900 °C for 12 h in air to remove adsorbed water and carbon dioxide. Then they were mixed and ball milled with ethyl alcohol for 6 h, and calcinated at 600 °C for 12 h in air. The calcinated powders were ball milled again for 6 h. The precursor powders obtained then mixed with 3–18 wt.% Ag_2O and ball milled with ethyl alcohol for 6 h again. The resulting powders were compacted into pellets by cold isostatic pressing, sintered in air at 1100 °C for 12 h at a heating rate of 2 °C/min (Attempts to obtain the higher density samples, the pellets must stay at 300 °C for 2 h for the exothermic chemical reactions of Ag_2O decomposition observed in Fig. 1.), and cooled to room

---

* Corresponding author. Tel.: +86 29 88494463; fax: +86 29 88492642.
E-mail addresses: liuxiao327@163.com (X. Liu), hqfan3@163.com (H. Fan).

0025-5408/$ – see front matter © 2012 Elsevier Ltd. All rights reserved.
http://dx.doi.org/10.1016/j.materresbull.2012.10.012

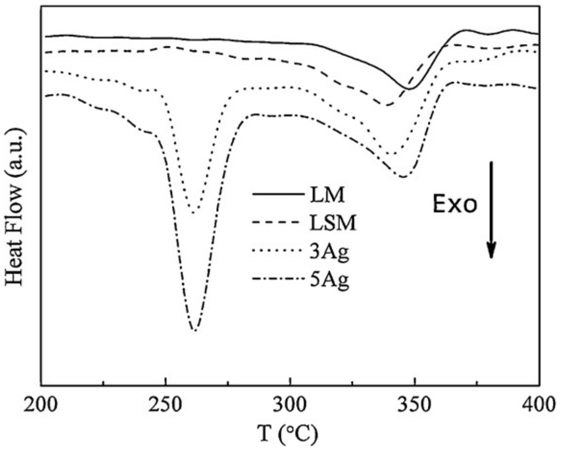

Fig. 1. DTA curves of the precursor powders LM-5Ag in air.

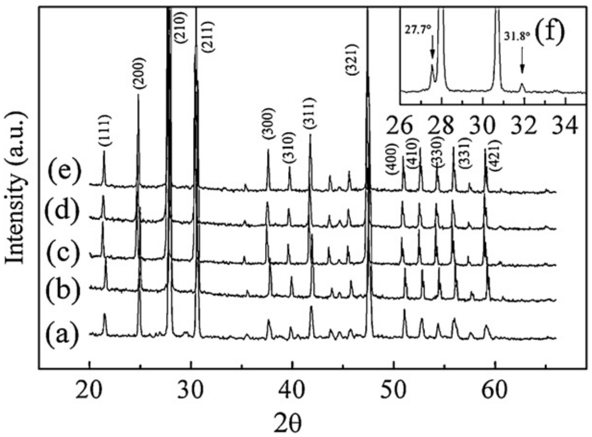

Fig. 2. XRD patterns of the $La_2Mo_2O_9$ based ceramics sintered in air at 1100 °C. (a) LM, (b) LSM, (c) 3Ag, (d) 5Ag, (e) 8Ag, and (f) 15Ag.

temperature naturally. After that, the pellets obtained were about 8.8 mm in diameter and 1.2 mm in thickness.

Phase structure of the sintered pellets was investigated by X-ray diffraction (XRD) (XRD-7000, Shimadzu, Kyoto, Japan) with Cu Kα radiation and 2θ ranges from 10° to 80°. Morphologies of natural surface of the sintered pellets were observed by field-emission scanning electron microscopy (FE-SEM) (JEOL-6700F, Japan Electron Co., Tokyo, Japan) with energy-dispersive X-ray spectroscope instrument (EDS) operated at 20 kV. Transmission electron microscopy images and selected area electron diffraction patterns were obtained using a high resolution transmission electron microscopy (TEM; JEM-3010, QUESTAR, New Hope, USA). Thermal analyses were performed on pellets by using thermo-gravimetric analysis (DTA/DSC) (Q600-SDT, TA Instruments Ltd., West Sussex, UK) with a TA instruments apparatus under air flow (heating/cooling rate of 10 °C/min). X-ray photoelectron spectroscopy (XPS) measurements were obtained by using a spectrometer (VG ESCALAB220i-XL, Thermo Scientific, MA, USA). The sintered pellets were polished for property investigations. Silver electrodes were coated on both polished surfaces and fired at 850 °C for 30 min to form a metal-insulator-metal (MIM) capacitor. The weak-field dielectric response with the signal level of 500 mV/mm was measured by using a precision impedance analyzer (4294A, Agilent, CA, USA) associated with temperature controller (TP94, Linkam, Surrey, UK) in the frequency range of 100 Hz to 10 MHz and temperature range of 30–600 °C at the heating rate of 3 °C/min.

3. Results and discussion

As a prerequisite, DTA was carried out to probe the thermal stability of raw powder sample. Thermodynamic studies have suggested that the Ag^0 is more stable than Ag_2O at temperatures of $>$189.8 °C in air [19]. The DTA curves of precursor powders reported in Fig. 1 shows that an extra exothermic peak was measured in 3Ag and 5Ag in the temperature range from 200 °C to 400 °C compared with LM and LSM. The peak at about 260 °C in 3Ag and 5Ag is due to the exothermic chemical reactions of Ag_2O decomposition. Therefore, the precursor powders stayed at this temperature for 2 h in order to remove oxygen at this stage to prevent tiny defects and cracks on the ceramics calcinated. The exothermic peak at about 350 °C is for the oxides reaction and after that the LM phase is formed gradually.

XRD patterns of LM-15Ag are shown in Fig. 2. Although $La_2Mo_2O_9$ is reported to be monoclinic phase at low temperature, its distortion from cubic symmetry is too small to be observed in a regular diffractogram. As shown in the figure, it can be concluded that all the samples have no such splitting diffraction peak and are in good agreement with cubic phase when Ag_2O addition less than 15 wt.%. A small impurity diffraction peak appears at around $2\theta = 27.7$, 31.8 in 15Ag samples. For samples (a)–(e), all the characteristic peaks moved slightly, and the migration tendency is similar to that in the LSM series [20]. When a small amount of Sr^{2+} enter into the lattice, it mainly occupy the A site. The consequent oxygen vacancy increased with the increase of aliovalent substitutions. With doping concentration further increasing, the blocking effects of defect dipoles are formed, displaying right shift in XRD. Moreover, all the XRD results with high intensity of diffraction peak exhibit higher crystallinity.

No appreciable pores and impurity phase at the grain boundaries are observed from the SEM images for the series 3Ag–10Ag, shown in Fig. 3 except for 12Ag, where there are extensive porosity and cracks on the ceramics. The densities of the samples with Ag addition are all higher than that in the LM and LSM ceramics, more than 91% of the theoretical density. The results of EDS certify that there is hardly any silver element on the free surfaces of silver addition ceramics. This may result from silver evaporation at the high temperatures. There are no impurity peaks found in XRD diffraction patterns, indicating that the silver is chemically stable in $La_2Mo_2O_9$ despite the relatively high anneal temperature, which is in agreement with previously reported [18]. In Fig. 4, the presence of a strong endothermic peak around 580 °C in DSC curves signatures the order–disorder transition in LM and LSM. The absence of this structural transition in the 3Ag–8Ag samples unequivocally confirms the suppression of order–disorder transition and consequent stabilization of the high temperature cubic phase at room temperature. As well, we can conclude that more heat was released as a result of Ag addition from the DSC results.

The structural change and electrical properties of LM were studied in detail for the phase transition. Fig. 5 illustrates the temperature dependence of the real part of dielectric permittivity (ε') and the dielectric loss ($\tan\delta$) for the series ceramics. At the lower temperature below 200 °C, the dielectric permittivity is considered as the intrinsic contribution. As the temperature increased, the dielectric permittivity increases by several orders of magnitude for the localized charge carriers hopping between spatially fluctuating lattice potentials. In Fig. 5, there are two obvious dielectric anomalies,corresponding to respective oxygen ion diffusion process: O(1)–O(3), O(1)–O(2), in all the ceramics except for LM, where there is only one relaxation peak, corresponding to O(1)–O(3) diffusion. This phenomenon coincides with the LSM series. The dielectric characteristics in sliver added